

# Complexation of *p*-Sulfonatocalixarenes with Local Anaesthetics Guests: Binding Structures, Stabilities, and Thermodynamic Origins

Qian Li,<sup>[a]</sup> Dong-Sheng Guo,<sup>[a]</sup> Hai Qian,<sup>[a]</sup> and Yu Liu\*<sup>[a]</sup>

**Keywords:** Calixarenes / Drug delivery / Host-guest systems / Conformation analysis / Thermodynamics

The binding geometries, abilities and thermodynamic parameters for the intermolecular complexation of three water-soluble *p*-sulfonatocalix[*n*]arenes (**SC $n$ As**), *p*-sulfonatocalix[4]arene (**SC4A**), *p*-sulfonatocalix[5]arene (**SC5A**), and *p*-sulfonatothiacalix[4]arene (**STC4A**), with five local anaesthetics (**LA**), procaine, tetracaine, lidocaine, dibucaine, and procainamide, have been determined by means of <sup>1</sup>H NMR spectroscopy, X-ray crystallography, and isothermal titration calorimetry (ITC). The obtained results show that the complexation of **SC $n$ As** with **LA** guests shows unappreciable

guest selectivity, but regular host selectivity: **SC4A** > **SC5A** > **STC4A** for each guest. A large difference in the enthalpy term is responsible for the decrease in the stability constants. The intrinsic relationship between binding structures and host selectivities were comprehensively analyzed and discussed from the viewpoint of thermodynamics. Furthermore, the complexation of **SC4A** towards **LA** guests were compared with other macrocyclic hosts,  $\beta$ -cyclodextrin and cucurbit[7]uril.

## Introduction

Calixarenes,<sup>[1]</sup> composed of phenolic units linked by methylene groups, represent one of the most widely studied classes of organic supramolecular hosts, and are described as “macrocycles with (almost) unlimited possibilities” due to their capacity for facile modification. As a typical class of water-soluble calixarene derivatives, *p*-sulfonatocalix[*n*]arenes (**SC $n$ As**, *n* = 4–8), are endowed with water solubility and biological compatibility.<sup>[2]</sup> Possessing three-dimensional, flexible,  $\pi$ -rich cavities, the **SC $n$ As** family are capable of versatile complexation with a range of guest molecules, including inorganic cations,<sup>[3]</sup> neutral molecules,<sup>[4]</sup> organic ammonium cations,<sup>[5]</sup> pyridiniums/viologens,<sup>[6]</sup> and even biological or pharmaceutical molecules.<sup>[7]</sup> All these outstanding properties enable **SC $n$ As** to open up highly diverse applications in molecular recognition/sensing,<sup>[8]</sup> crystal engineering,<sup>[9]</sup> catalysis,<sup>[10]</sup> amphiphiles,<sup>[11]</sup> and some other biomedical applications.

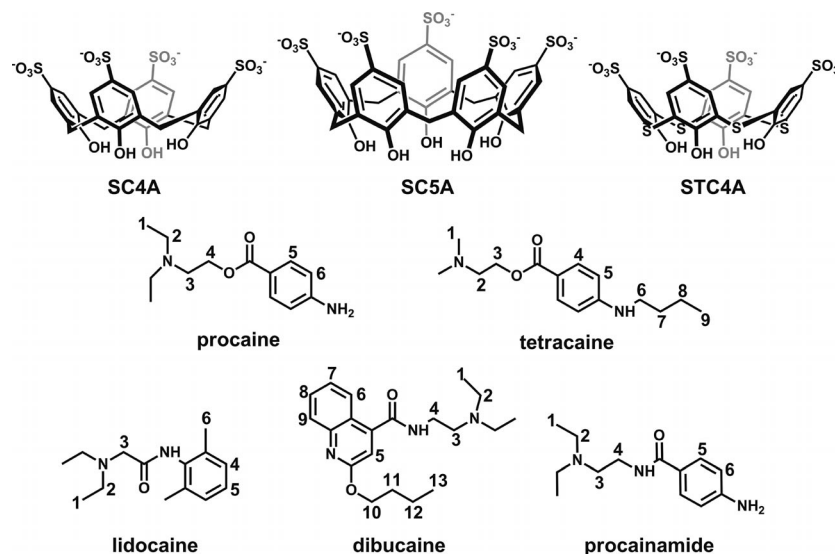
The biochemistry of **SC $n$ As** has been rapidly developed during the past two decades, especially with respect to their pharmaceutical applications, in particular, complexation of pharmacologically active compounds. Such host–guest complexes have been investigated in view of their potential use as new therapeutic formulations, designed to increase the bioavailability and/or to decrease the systemic toxicity

of the biologically active compounds.<sup>[12]</sup> Coleman et al. proposed the use of **SC $n$ As** as generic cocrystal formers to increase the aqueous solubility of the Active Pharmaceutical Ingredients of drugs.<sup>[13]</sup> Yang et al. reported the use of **SC $n$ As** to produce stable complexes with improved bioavailability for nifedipine, a calcium-channel blocker, which is practically insoluble in water.<sup>[14]</sup> Moreover, they discovered that simultaneous oral ingestion of the **SC $n$ As** (*n* = 6 and 8) significantly increased the bioavailability of the drug after oral administration in male Sprague–Dawley rats. In previous work, we proposed a new therapeutic protocol for treatment of paraquat poisoning, in which **SC5A**, administered orally, could pronouncedly decrease the mortality rate and mitigate the damage in the lung and liver.<sup>[15]</sup> Additionally, we investigated the complexation behavior of a complex between **SC4A** and topotecan, which is a chemotherapy agent that is a topoisomerase I inhibitor, and conducted an aqueous solubility study that shows that **SC4A** enhanced the water-solubility of topotecan.<sup>[16]</sup> We also explored the inclusion complex of **SC4A** with irinotecan (**CPT-11**), and experimental results showed that the complexation of **CPT-11** with **SC4A** increases the antiproliferative activity of **CPT-11**.<sup>[17]</sup>

Local anaesthetics (**LA**), used for topical administration, are intended to relieve such discomfort sensations as pain, itching, and burning associated with minor surgical operations, dermatological disorders, etc., which are characterized by limited duration of analgesia.<sup>[18]</sup> The drugs alleviate the unpleasant sensations by causing reversible inhibition of axonal voltage-gated sodium channels responsible for depolarization and thus prevent or diminish the conduction of sensory nerve impulses near to the site of their appli-

[a] Department of Chemistry, State Key Laboratory of Elemento-Organic Chemistry, Nankai University, Tianjin 300071, P. R. China  
Fax: +86-22-2350-3625  
E-mail: yuliu@nankai.edu.cn

Supporting information for this article is available on the WWW under <http://dx.doi.org/10.1002/ejoc.201200515>.

Scheme 1. Structural illustration of *SCnA* hosts, and *LA* guests.

cation.<sup>[19]</sup> In order to improve the applications of *LA*, the inclusion complexation of a series of *LA* agents (Scheme 1) has been systematically studied with cyclodextrin (*CD*)<sup>[20]</sup> and cucurbituril (*CB*)<sup>[21]</sup> macrocycles. However, the inclusion behavior of *LA* agents and *SCnAs* has only been occasionally reported. Fernandes and co-workers reported the complexation between tetracaine/proprilocaine and *SC6A*.<sup>[22]</sup> Coleman and co-workers outlined conformational isomerism in the solid-state structures of tetracaine with *SC4A*.<sup>[23]</sup> Therefore, in this work, we wanted to study the binding behavior of *SCnAs* toward *LA* guests, and comprehensively discuss their inclusion geometries, complexation stabilities, and thermodynamic origins. Moreover, the complexation of *SC4A* towards *LA* guests, compared with other macrocycles,  $\beta$ -*CD* and *CB*[7], were provisionally performed.

Three smaller host analogues (Scheme 1), *SC4A*, *SC5A*, and *p*-sulfonatothiacalix[*n*]arene (*STC4A*) were selected because of their relatively stable, preorganized cone shapes. *SC4A* possesses the most compact framework and relatively high  $\pi$ -electron density, whereas *SC5A* is generally regarded as the largest and least rigid host. Compared to *SC4A*, *STC4A* is less electron-rich and has an enlarged hydrophobic cavity, with a greater degree of flexibility of the framework, and additional binding sites.

*LA* guests are classified by an ester or amide link between a hydrophilic amine end and a lipophilic aromatic end. In this content, amide-linked *LAs* include dibucaine, lidocaine, and procainamide, and ester-containing *LAs* cover procaine and tetracaine.

Considering the effects of pH on both hosts and guests, experiments were conducted to analyze the host–guest binding structures under acidic and neutral conditions. The discussion on complexation stability and thermodynamics, however, mainly relates to physiological conditions at pH 7.2, due to the requirements for clinical drug administration.

## Results and Discussion

### Binding Structures in the Solid State

Single-crystal X-ray diffraction analyses supplied quantitative information for five complexes of *SCnAs* with *LA* guests in the solid state. These five complexes were obtained in their monocrystalline forms by applying the method of solvent volatilization at pH 2.0. Complexes procainamide  $\subset$  *SC4A* and procaine  $\subset$  *SC5A* crystallized in the monoclinic space group  $P2_1/c$ , and other complexes procaine  $\subset$  *SC4A*, procainamide  $\subset$  *STC4A* and tetracaine  $\subset$  *STC4A* crystallized in the triclinic space group  $P\bar{1}$ . The asymmetric units contain the following: one crystallographically distinct *SC4A*, two procainamide, and 18.7 water molecules for procainamide  $\subset$  *SC4A*; one *SC4A*, two procaine, and 11.63 water molecules for procaine  $\subset$  *SC4A*; one *SC5A*, two procaine, and 11.5 water molecules for procaine  $\subset$  *SC5A*; one *STC4A*, two procainamide, and 6.25 water molecules for procainamide  $\subset$  *STC4A*; one *STC4A*, two tetracaine, and 15.5 water molecules for procainamide  $\subset$  *STC4A*. Among these crystals, some carbon atoms of procaine in complex procaine  $\subset$  *SC5A*, some sulfonate groups of *SCnAs*, and several water molecules are disordered at two or more positions. Unfortunately, it was not possible to locate all hydrogen atoms from the Fourier difference map for this to be clarified.<sup>[24]</sup>

In complex procainamide  $\subset$  *SC4A*, one procainamide guest penetrates into the *SC4A* cavity with a slantwise orientation (Figure 1), whereas the other acts as a counterion located in the crystal lattice. The triethylammonium group of procainamide is captured into the cavity of *SC4A* through four C–H $\cdots$  $\pi$  interactions {C36–H36 $\cdots$ ring of C8–13 [3.827(4) Å, 166.4(1)°]; C37–H37 $\cdots$ ring of C1–6 [3.704(9) Å, 144.3(2)°]; C38–H38 $\cdots$ ring of C15–20 [3.224(5) Å, 126.2(2)°]; C39–H39 $\cdots$ ring of C22–27 [2.822(0) Å, 154.2(9)°]}, and two unconventional hydrogen

bonds {C41...O14 [3.287(7) Å and 138.7(7)°]; C40...O15 [3.658(6) Å and 124.4(5)°]}, whereas the amide linkage is fixed at the upper rim of **SC4A**, captured by one sulfonate group through a hydrogen bond {N2...O8 [2.847(6) Å, 160.1(0)°]}.

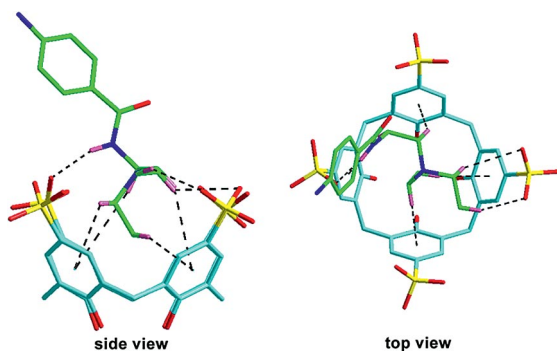


Figure 1. Solid-state inclusion structure of procainamide  $\subset$  **SC4A**. The broken lines represent the intermolecular hydrogen bonds or the C–H... $\pi$  interactions between host and guest. The other guests, water molecules, and hydrogen atoms are omitted for clarity.

In complex procainamide  $\subset$  **STC4A**, one procainamide guest is included in the **STC4A** cavity, whereas the second acts as a counterion in the crystal lattice (Figure 2). The triethylammonium moieties of the procainamide are immersed into the cavity of **STC4A** in a slantwise manner through three C–H... $\pi$  interactions {C96–H96...ring of C19–24 [2.925(0) Å, 152.8(5)°]; C99–H99...ring of C13–18 [3.106(5) Å, 110.8(9)°]; C100–H100...ring of C1–6 [2.798(8) Å, 134.7(9)°]}, two unconventional hydrogen bonds {C95...O5 [3.260(3) Å, 97.6(9)°]; C98...O13 [3.414(8) Å, 136.7(9)°]}, and one hydrogen bond {N11...O14 [2.950(4) Å, 161.2(6)°]} between the amide linkage and sulfonate group. To accommodate the guest well, **STC4A** adopts a distorted  $C_{2v}$  symmetry conformation with S...S distances of trans sulfonate groups of 11.780(6) Å and 9.461(0) Å, which is different from  $C_{4v}$  cone shape **SC4A** with S...S distances of 10.242(2) Å and 10.589(2) Å in procainamide  $\subset$  **SC4A**. Compared to the accommodation of procainamide in a lightly acclivitous manner in complex procainamide  $\subset$  **SC4A**, the guest molecule is more slantways encapsulated into the cavity of **STC4A**, close to horizontal orientation. This structure difference can be ascribed to the replacement of bridging atoms from methylene to sulfide linkage, which brings about a 15% enlargement of the cavity size and enables the host to accommodate most of the volume of the guest molecule.<sup>[4c,25]</sup>

In complex tetracaine  $\subset$  **STC4A**, one tetracaine guest is slantways encapsulated into the cavity of **STC4A** with the butylanilinium immersed, and the second is restricted in the crystal lattice as a counterion. The binding mode differs from tetracaine  $\subset$  **SC4A** in which the dimethyl ammonium cationic end group is included into the **SC4A** cavity.<sup>[23]</sup> This discrepancy between **STC4A** and **SC4A** complexes could be attributed to different cavity sizes and crystal growing conditions. Different types of noncovalent interactions between **STC4A** and tetracaine were also observed (Figure 3),

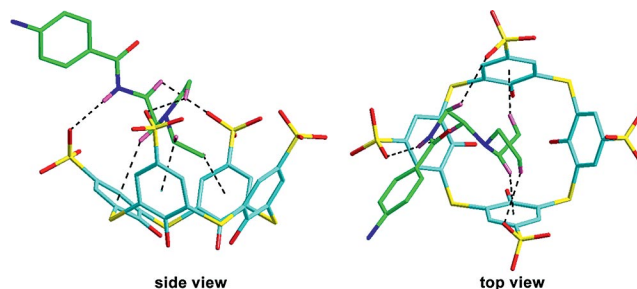


Figure 2. Solid-state inclusion structure of procainamide  $\subset$  **STC4A**. The broken lines represent the intermolecular hydrogen bonds or the C–H... $\pi$  interactions between host and guest.

including two C–H... $\pi$  interactions {C38–H38...ring of C13–18 [3.055(7) Å, 109.2(8)°]; C39–H39...ring of C7–12 [2.794(7) Å, 123.3(8)°]}, and three unconventional hydrogen bonds {C28...O15 [3.199(1) Å and 112.2(4)°]; C36...O14 [3.499(5) Å and 145.6(3)°]; C37...O8 [3.491(6) Å and 161.0(6)°]}. In comparison with complex procainamide  $\subset$  **STC4A**, **STC4A** in tetracaine  $\subset$  **STC4A** adopts more pinched-cone conformation with S...S distances of 12.539(2) Å and 8.536(0) Å, respectively.

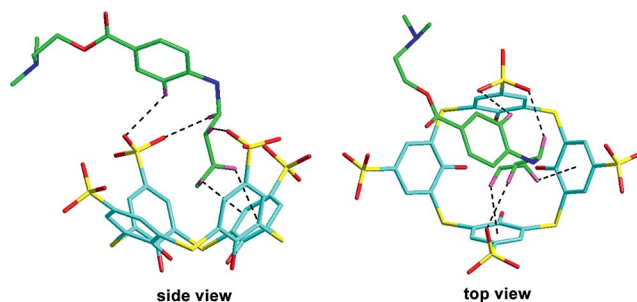


Figure 3. Solid-state inclusion structure of tetracaine  $\subset$  **STC4A**. The broken lines represent the intermolecular hydrogen bonds or the C–H... $\pi$  interactions between host and guest.

Replacement of the amide linkage of procainamide by the ester bond of procaine leads to the disappearance of the hydrogen bond between the amide hydrogen and sulfonate oxygen. This eventually causes a more vertical orientation of the aniline group in the procaine  $\subset$  **SC4A**, compared with procainamide  $\subset$  **SC4A**. As shown in Figure 4, procaine adopts an almost L-shaped conformation, with the aliphatic moiety located in the cavity of **SC4A**. The aromatic group is located apart from the cavity at a nearly parallel orientation to the axis of the cavity. One ethyl arm in the aliphatic moiety points outside the **SC4A** cavity, whereas the second points inside the cavity. This complex is stabilized by three unconventional hydrogen bonds {C90...O26 [3.439 Å, 165.6(8)°]; C92...O18 [3.815 Å, 122.1(1)°]; C93...O30 [3.992 Å, 117.7(4)°]} and three C–H... $\pi$  interactions {C91–H91...ring of C36–41 [3.311(3) Å, 174.6(8)°]; C94–H94...ring of C43–48 [2.653(3) Å, 143.2(1)°]; C95–H95...ring of C29–34 [2.828(9) Å, 119.4(0)°]}. In complex procaine  $\subset$  **SC5A** (Figure 5), the aromatic plane of the guest molecule is in a slantwise orientation outside the cavity of **SC5A** with two unconventional

hydrogen bonds {C71...O18 [3.347(7) Å, 94.6(2)°]; C72...O19 [3.624(1) Å, 116.9(1)°]}. Two ethyl arms of the aliphatic moiety point inside the **SC5A**, which are stabilized by three C–H... $\pi$  interactions {C81–H81...ring of C15–20 [2.626(7) Å, 148.2(9)°]; C82–H82...ring of C8–13 [2.835(9) Å, 156.8(0)°]; C83–H83...ring of C1–6 [2.961(6) Å, 139.3(9)°]}. The remaining interaction between **SC5A** and procaine is a hydrogen bond {N2...O20 [2.756(1) Å, 158.6(5)°]}, which can be explained as the more flexible cone-shaped conformation of the **SC5A** cavity. This structural distinction compared with procaine  $\subset$  **SC4A** can be ascribed to the fact that the cavity of **SC5A** is wider; thus, **SC4A** has a bowl-shape, whereas **SC5A** can be regarded as a shallow-dish shape.

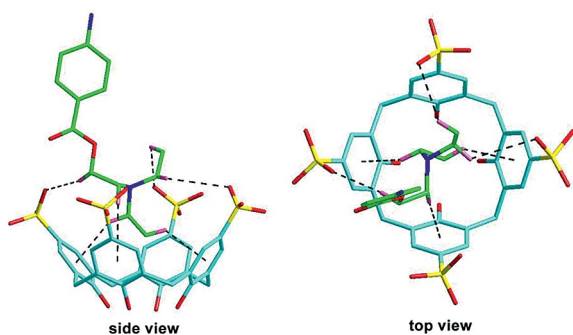


Figure 4. Solid-state inclusion structure of procaine  $\subset$  **SC4A**. The broken lines represent the intermolecular hydrogen bonds or the C–H... $\pi$  interactions between host and guest.

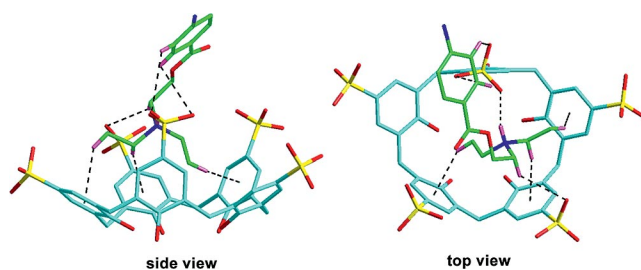


Figure 5. Solid-state inclusion structure of procaine  $\subset$  **SC5A**. The broken lines represent the intermolecular hydrogen bonds or the C–H... $\pi$  interactions between host and guest.

### Host–Guest Binding Behavior in Solution

NMR spectroscopy is a powerful tool that can be used to determine the structures of calixarene complexes by analyzing complexation-induced shifts.<sup>[5a]</sup> Herein, to gain detailed information about the complex structures of **SCnAs** with the five LA guests, we recorded relevant <sup>1</sup>H NMR spectra in both pD 2.0 and 7.2 phosphate buffer solutions. In general, the signals of the guest protons often underwent pronounced upfield shifts owing to the ring current effect of the aromatic nuclei of calixarenes upon complexation. All of the guests in the present study, in both acidic and neutral solutions, exhibit fast exchange between the free and included forms on the NMR time-scale.<sup>[5c]</sup> The chemical shift changes are presented in the Supporting Infor-

mation (Tables S1–4), and can be used as powerful evidence for the host–guest binding geometries. According to different protonated forms of LA guests and their binding modes with **SCnAs**, the five complexes can be divided into three species: procaine and procainamide  $\subset$  **SCnAs**, dibucaine and tetracaine  $\subset$  **SCnAs** and lidocaine  $\subset$  **SCnAs**.

As shown in the Supporting Information (Table S1), in the presence of approximately 1 equiv. **SC4A** in acidic or neutral conditions, the protons H1–4 of procaine undergo pronounced upfield shifts (H1 > H2 > H3 > H4), with negligible shifts for H5 and H6, indicating that the triethylammonium moiety is exclusively encapsulated into the cavity of **SC4A**. This may be compared with the behavior of procaine with **CB[7]** and  $\beta$ -CD.<sup>[20b,21]</sup> The monocationic form of the guest is postulated to bind with the aromatic amine and ester groups within the cavity of  $\beta$ -CD, and to encapsulate the triethylammonium group with **CB[7]**, respectively. According to complexation-induced shifts of procaine protons by **SC5A** in both acidic and neutral conditions, protons shift upfield in the order of H2 > H3 > H1 > H4 > H5 > H6. This means that the aliphatic chain of the guest immerses into the cavity of **SC5A**, with the aromatic moiety staying in a less acclivitous orientation than that in **SC4A**.<sup>[6c]</sup> These deduced complex structures were verified by previous studies on complexes procaine  $\subset$  **SC4A** and procaine  $\subset$  **SC5A**. The  $\Delta\delta$  values of procaine protons in the case of **SC4A** complex imply a similar encapsulation mode to those of the previous two. For the procainamide guest encapsulated by **SCnAs** under the two conditions, similar binding modes were deduced according to <sup>1</sup>H NMR measurements. Taking the order of  $\Delta\delta$  values of triethylammonium portions into account, we can infer that H2 suffers from the ring current effect of the aromatic nuclei to a greater extent in the case of **SC5A**. This phenomenon can be attributed to the order of cavity sizes (**SC4A** < **STC4A** < **SC5A**), which makes the ethyl group more incumbent into the cavity of **SC5A** than **SC4A** or **STC4A**. It should be mentioned here that the protonation states of guests are different under acidic and neutral conditions; two-positive charged form for both procainamide and procaine at pD 2.0, and one-positive charged form at pD 7.2. However, this does not lead to a clear difference in the mode of binding – only to chemical shift changes.

The dibucaine guest displays different binding modes under acidic and neutral conditions. In neutral solution, dibucaine is in monocationic form with the triethylammonium group protonated. As shown in the Supporting Information (Table S2), the <sup>1</sup>H NMR spectra of complexes of dibucaine with **SCnAs** clearly reveal large upfield shifts of the H1–H4 protons, with negligible shifts of the butyl and quinolyl protons, suggesting that **SCnAs** tend to include the positive alkyl ammonium moiety of dibucaine. In acidic solution, both quinolyl and triethylammonium groups are protonated, giving the dicationic form of dibucaine, according to the  $pK_a$  values.<sup>[21]</sup> Upon addition of **SC4A**, the sequence of  $\Delta\delta$  values is H1 > H2 > H3 > H4 in the triethylammonium group, H8 > H7 > H6 > H9 > H5 in the quinolyl group, and H13  $\approx$  H12  $\approx$  H11 > H10 in the butyloxy group. Upon ad-

dition of **SC5A**, the sequence of  $\Delta\delta$  values is  $H2 > H1 > H3 > H4$  in the triethylammonium group,  $H8 \approx H7 \approx H6 > H9 \approx H5$  in the quinolyl group, and  $H13 \approx H12 \approx H11 > H10$  in the butyloxy group. The complexation-induced shifts of dibucaine  $\subset$  **STC4A** were not obtained owing to the poor water-solubility of the complex. Commonly, larger  $\Delta\delta$  values indicate the portion of guest more deeply immersed in the cavity of **SCnAs**. Consequently, we can deduce that **SC4A** binds either the triethylammonium moiety or the butyloxy group without regioselectivity, and that the quinolyl moiety should be included into the cavity of **SC4A** near the upper rim (Figure 6); the same should also occur in the complexation of dibucaine with **SC5A**.

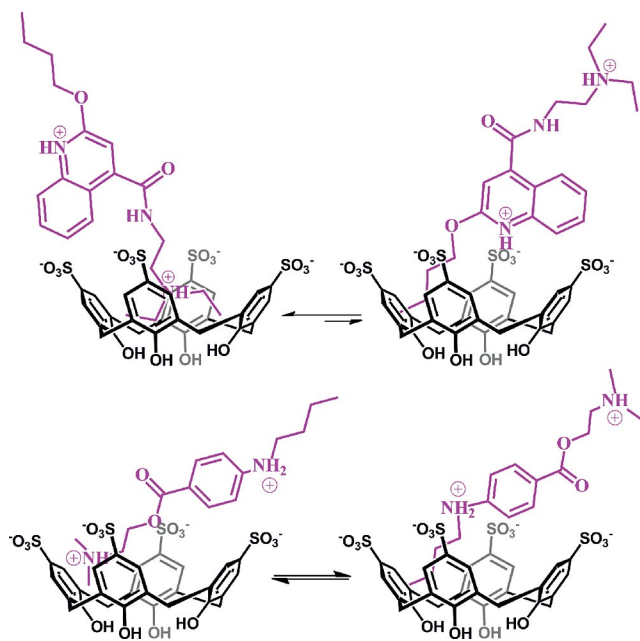


Figure 6. The deduced binding equilibria of **SC4A** with dibucaine (upper) and **SC4A** with tetracaine (lower) under acidic conditions.

Similar results can also be observed in the tetracaine  $\subset$  **SCnA** complexes. As shown in the Supporting Information (Table S3), a binding equilibrium can be deduced in which either the tertiary ammonium moiety or the butylanilinium group could enter into the **SC4A** cavity with no regioselectivity under acidic conditions (Figure 6). With regard to **SC5A**, tetracaine adopts an accumbent binding manner within it; this is characteristic for a shallow immersion on the trimethylammonium portion either under acidic or neutral conditions. In the case of **STC4A**, unfortunately, owing to the poor solubility of the tetracaine complex with **STC4A** under acidic conditions, we could not obtain a  $^1\text{H}$  NMR spectrum and only the crystal structure (Figure 3) could be used to deduce its bonding mode. Under neutral conditions, it could be observed that the  $\Delta\delta$  values of protons H6–9 are larger than other guest protons, indicating that **STC4A** tends to capture the butyl group, the encapsulation mode of which is similar to that found in the crystal structure.

Lidocaine exists exclusively in the monocationic form in both acidic and neutral solutions; protonation occurs at the tertiary amine of guest molecule. However, with the solution adjusted from acidic to neutral (basic), some of the phenolic hydroxyl groups of the **SCnAs** begin to become deprotonated<sup>[26]</sup> and, therefore, the cavities of the calixarenes become more strongly electron-donating. **SCnAs** are prone to encapsulate the positive charge moiety of the guest, according to the aforementioned discussion on binding sites of **SCnAs** with other **LA** guests. As can be seen in the Supporting Information (Table S4), in the case of **SC4A** with lidocaine, similar binding modes can be deduced under both acidic and neutral conditions. However, **SC5A** provides a binding geometry that is distinct from that of the guest with **SC4A**. According to complexation-induced shifts of lidocaine protons by **SC5A**, the guest may adopt an accumbent encapsulation mode under acidic conditions; whereas in neutral solution, the  $\Delta\delta$  values of H1–3 increase quickly, accompanied with a decline of the  $\Delta\delta$  values of H4–6, which can be ascribed to the enhanced attraction between the cationic portion and the deprotonated phenolic hydroxyl groups, leading to a deeper immersion of the tertiary ammonium.

Examining all the encapsulation modes of the five **LA** guests, on one hand, **SC4A** and **SC5A** tend to bind the positive charged alkyl ammonium moiety under neutral conditions, although, **STC4A** prefers to bind to the nonprotonated, hydrophobic butyl group of tetracaine; on the other hand, it should be mentioned that the different cavity sizes of **SCnAs** contribute to the distinct binding modes; for instance, the larger the cavity size, the closer to the accumbent orientation for guest encapsulation. This may be contrasted with the behavior of these **LA** guests with **CB[7]**, in which the monocationic forms of procaine, procainamide and dibucaine guests are found to bind exclusively with the triethylammonium groups within the hydrophobic cavity, leaving the neutral portions outside of the cavity near the portal.<sup>[21]</sup> While for the inclusion behavior of monocationic procaine with  $\beta$ -**CD**, a completely contrary binding mode is postulated in which the nonprotonated group is bound and the positive charged moiety lies outside.<sup>[20e]</sup> It is clear for inclusions of monocationic guests with **CB[7]** that the observed separation of the  $^1\text{H}$  NMR resonances of the non-equivalent diastereotopic  $\text{CH}_2$  protons of the terminal ethyl groups on the prochiral protonated nitrogen could be attributed to nonequivalent local environments experienced within the cavity upon **CB[7]** inclusion of these guests. However, for inclusion of the **LA** guests in **SCnAs**, similar phenomena for  $\text{CH}_2$  protons of terminal ethyl groups under nonequivalent local environments were not observed, owing to fast exchange between the free and complexed guest on the NMR time-scale. In acidic media, **SCnAs** prefer to accommodate triethylammonium portions of procaine and procainamide with the anilinium group close to the negative sulfonate groups; this host also tends to bind the two positive sites of tetracaine, whereby the encapsulation equilibrium can be postulated to explain the complexation process. However, **CB[7]** was prone to thread on these three guest

molecules initially from one positive site and then to approach the second protonation site, with these two positive charges eventually locating near two restrictive portals. In the case of dibucaine, **SC4A** and **SC5A** tend to bind all of the triethylammonium, butyl and aromatic groups; by contrast **CB[7]** displays no apparent affinity for the aromatic moiety of the molecule but for triethylammonium and butyl groups in acidic solution.

As previous studies without guest molecules have shown, the methylene protons in either **SC4A** or **SC5A** give a single NMR peak assigned to a rapid cone-to-cone interconversion of uncomplexed host, indicating that the host sulfonatocalixarenes exists in a flexible conformation. However, after complexation with guests, this single peak of **SC4A** broadens to the baseline or splits into two sets of double peaks with the same integration intensities, which means that **SC4A** adjusts itself into a more fixed cone conformation to adopt the size of the guest molecule; thus, the conformation changes of the host become slow on the NMR time-scale following the inclusion of guest.<sup>[6b]</sup> In contrast, the NMR signal assigned to the methylene protons in **SC5A** remain in their original shape after complexation with guest molecules, which means that the conformation of **SC5A** remains flexible during the course of complexation, presumably due to its larger size and higher intrinsic flexibility. For **STC4A**, which has a more flexible cone compared to **SC4A** and is more rigid compared to **SC5A**, NMR spectra cannot directly reveal any conformational change due to the lack of bridgehead  $-\text{CH}_2-$  protons. The distinguishable conformational freedoms between **SC4A**, **SC5A**, and **STC4A** can be well-reflected by the thermodynamic parameters of the entropy term (see below).

### Binding Ability and Thermodynamics

To investigate quantitatively the inclusion complexation behavior of **SCnAs** with **LA** guests and their thermodynamic origins, isothermal titration calorimetry (ITC) experiments were performed in phosphate buffer solution (pH 7.2), which is a powerful tool for determining host–

guest complex interactions, because it not only gives the complex stability constants ( $K_S$ ), but also yields their thermodynamic parameters (enthalpy and entropy changes  $\Delta H^\circ$ ,  $\Delta S^\circ$ ). Quantitative data obtained are listed in Table 1. In all cases, the titration data could be fit well by computer simulation by using the “one set of binding sites” model and repeated as 1:1 complex formation; the 1:1 binding modes for some inclusion complexes have also been validated by their crystal structures, therefore, higher-order complexes were not considered further.

It is well-documented that, among several weak noncovalent interactions working between **SCnAs** and guests, the charge interactions,<sup>[27]</sup> hydrogen bond,  $\pi$ -stacking,  $\text{C}-\text{H}\cdots\pi$  and van der Waals interactions mainly contribute to the enthalpy changes, whereas the conformation change and desolvation effect contribute to the entropy changes.<sup>[28]</sup> As can be seen in Table 1, all of the intermolecular complexation processes between **SCnAs** and **LA** guests are entirely driven by the favorable enthalpy changes ( $\Delta H^\circ = -18.05 \approx -34.21 \text{ kJ mol}^{-1}$ ), accompanied either by unfavorable entropy changes ( $T\Delta S^\circ = -0.06 \approx -13.26 \text{ kJ mol}^{-1}$ ) or by slightly favorable entropy change ( $T\Delta S^\circ = 0.13 \text{ kJ mol}^{-1}$ ). From the above crystal structure analyses and NMR investigations,  $\text{C}-\text{H}\cdots\pi$  interactions between the ammonium groups in **LA** guests and the aromatic cavities of calixarenes, charge interactions of the **LA** guest's cationic moiety with sulfonate groups, and hydrogen bonds between ester/amide or ammonium/aniline groups and sulfonate groups are the dominant driving forces that lead to exothermic enthalpy changes in the host–guest complexation. The sulfonate groups electrostatically attract organic ammonium cations, which causes a large degree of desolvation of the host and guest molecules, and then contributes to favorable entropy changes.<sup>[29]</sup> However, in most cases, the entropy terms are negative because the desolvation effect cannot compensate for the loss of conformational freedom. It is reasonable to suppose that the negative entropy changes mainly result from the loss of conformational degrees of freedom for the hosts and guests, and structural freezing upon complexation.

Table 1. Complex stability constants ( $K_S$ ), enthalpy ( $\Delta H$ ) and entropy changes ( $T\Delta S^\circ$ ) for 1:1 intermolecular complexation of **SCnAs** with **LA** guests in phosphate buffer solution (pH 7.2) at 298.15 K.

Host	Guest	$K_S [\text{M}^{-1}]$	$\Delta H^\circ [\text{kJ mol}^{-1}]$	$T\Delta S^\circ [\text{kJ mol}^{-1}]$
<b>SC4A</b>	procaine	$(5.09 \pm 0.08) \times 10^3$	$-33.71 \pm 0.28$	$-12.57 \pm 0.32$
	procainamide	$(1.02 \pm 0.01) \times 10^4$	$-34.21 \pm 0.11$	$-11.35 \pm 0.13$
	tetracaine	$(2.69 \pm 0.05) \times 10^3$	$-32.82 \pm 0.41$	$-13.26 \pm 0.45$
	lidocaine	$(6.56 \pm 0.06) \times 10^3$	$-32.55 \pm 0.21$	$-10.79 \pm 0.23$
	dibucaine	$(1.79 \pm 0.04) \times 10^4$	$-31.51 \pm 0.15$	$-7.26 \pm 0.22$
<b>SC5A</b>	procaine	$(1.63 \pm 0.01) \times 10^3$	$-26.07 \pm 0.16$	$-7.75 \pm 0.16$
	procainamide	$(1.78 \pm 0.02) \times 10^3$	$-27.13 \pm 0.06$	$-8.62 \pm 0.06$
	tetracaine	$(5.47 \pm 0.01) \times 10^2$	$-20.86 \pm 0.88$	$-5.25 \pm 0.90$
	lidocaine	$(1.12 \pm 0.02) \times 10^3$	$-22.76 \pm 0.10$	$-5.37 \pm 0.05$
	dibucaine	$(2.60 \pm 0.02) \times 10^3$	$-19.41 \pm 0.36$	$-0.06 \pm 0.37$
<b>STC4A</b>	procaine	$(6.23 \pm 0.01) \times 10^2$	$-23.11 \pm 0.14$	$-7.17 \pm 0.13$
	procainamide	$(6.49 \pm 0.02) \times 10^2$	$-21.55 \pm 0.08$	$-5.52 \pm 0.09$
	tetracaine	$(5.19 \pm 0.16) \times 10^2$	$-19.76 \pm 0.34$	$-4.29 \pm 0.41$
	lidocaine	$(7.70 \pm 0.05) \times 10^2$	$-24.88 \pm 0.18$	$-8.42 \pm 0.16$
	dibucaine	$(1.55 \pm 0.07) \times 10^3$	$-18.05 \pm 0.05$	$0.13 \pm 0.08$

The complexation of **SCnAs** with **LA** guests shows unappreciable guest selectivity, but regular host selectivity: **SC4A** > **SC5A** > **STC4A** for each guest. For the **SC4A** and **SC5A** pairs, the former bind the guests much tighter than the latter, and the host selectivities are in the range from 3 to 7 times. A close inspection of the calorimetric data revealed that a large difference in the enthalpy term is responsible for the decrease in the stability constants. These results are reasonable because the strength of the noncovalent interactions between **SCnAs** and guests is closely related to the distance, angle, the contact surface area between host and guest.<sup>[6d]</sup> Moreover, it is well-known that the intensity of C–H⋯π interactions, one of the most important intermolecular interactions between **SCnAs** and guests, depends to a large degree on π-electron density. Relative to **SC5A**, **SC4A** possesses a more compact framework and relatively higher π-electron density and, therefore, has better size-fit and more effective C–H⋯π interactions with the **LA** guests. The  $K_S$  values of **STC4A** decrease by almost one order of magnitude compared with those of **SC4A**, showing merely medium binding stability ( $K_S = 500\text{--}1500\text{ M}^{-1}$ ). Owing to the replacement of the methylene linkages of **SC4A** by sulfide, **STC4A** has certain inherent characteristics: wider cavity, lower π-electron density, and more flexibility. The weaker binding abilities of **STC4A** are mainly reflected in the enthalpy term as a result of less effective C–H⋯π interactions offered by the cavity of lower π-electron density. Meanwhile, the charge and hydrogen-bonding interactions between hosts and guests also contribute to the favorable enthalpy changes. However, these two interactions are not as dominant as the C–H⋯π interaction, which results in the differences in the enthalpy terms for the **SC4A**, **STC4A** and **SC5A** complexes. For example, **SC5A** possesses one more sulfonate group than **SC4A**, which favors formation of charge and hydrogen-bonding interactions with guests. However, in fact, the enthalpy terms of the **SC5A** complexes are not as favorable as those of the **SC4A** complexes.

It is also noted that intermolecular complexation of **SC4A** with **LA** guests exhibits most unfavorable entropy changes ( $T\Delta\Delta S^\circ = T\Delta S^\circ\text{SC4A} - T\Delta S^\circ\text{SC5A} = -2.73$  to  $-8.01\text{ kJ mol}^{-1}$ ;  $T\Delta\Delta S^\circ = T\Delta S^\circ\text{SC4A} - T\Delta S^\circ\text{STC4A} = -2.55$  to  $-8.97\text{ kJ mol}^{-1}$ ) among the three calixarene complexes. This originates from the large loss of degrees of system freedom, which includes the loss of conformational freedom for **SC4A** and **LA** guests. On one hand, **SC4A** undergoes the biggest loss of conformational freedom upon going from the flexible cone to the rigidified cone host–guest complex than does **SC5A/STC4A**.<sup>[4d,30]</sup> Such pronounced complexation-induced structure freezing of **SC4A** is also validated by the aforementioned NMR results (the signals of the bridging methylene protons change from a single peak to two peaks in the <sup>1</sup>H NMR spectra). On the other hand, the unfavorable entropy change is also due to freezing of motional freedom of the guest molecule upon complexation with the calixarene hosts.<sup>[31]</sup> There is increased loss of conformational freedom for the guest molecule after formation of the inclusion complex as the size of the host cavity decreases. Therefore, **LA** guests undergo the

largest conformational restriction when they penetrate into the **SC4A** cavity. Furthermore, based on the crystal structures, and the deduced binding geometry from NMR experiments, presumably, the **LA** guests adopt more slantways encapsulation in the cavity of **SC5A** and **STC4A** with the positive portion positioned close to the sulfonate rim, which leads to desolvation around the sulfonate groups. Therefore, the complexation of **SC5A** and **STC4A** are accompanied by less negative entropy changes.

Besides **SCnAs**, there have been numerous investigations on the complexation of **CDs** and **CBs** with **LA** guests. It is well-known that different macrocyclic hosts always show distinguishable inclusion affinities to substrates, because their structural characteristics and cavity properties differ significantly from each other. **CDs**, a family of macrocyclic oligosaccharides with six to eight D-glucose units ( $\alpha$ -,  $\beta$ -,  $\gamma$ -) linked by  $\alpha$ -1,4-glucose bonds, prefer to bind neutral or anionic guests over cationic species.<sup>[32]</sup> **CBs**, a family of novel pumpkin-shaped macrocyclic hosts, contain a hydrophobic interior cavity, with polar carbonyl groups surrounding the two restrictive portals, forming stable host–guest complexes with cationic guests.<sup>[33]</sup> For comparison purposes, in Table 2 we have summarized the host–guest stability constants for the 1:1 complex formation between the five **LA** guests and three macrocyclic hosts. The difference between **SC4A**,  $\beta$ -**CD**, and **CB[7]** was discussed in particular because they possess similar cavity sizes. The **SC4A** cavity (6.0–6.3 Å if approximated as a sphere)<sup>[4d]</sup> is comparable in diameter to the  $\beta$ -**CD** cavity (6.0–7.0 Å)<sup>[34]</sup> and the **CB[7]** cavity with a diameter of ca. 7.3 Å and a portal diameter of ca. 5.4 Å.<sup>[35]</sup> The stability constants of **SC4A** are almost one order of magnitude larger than those of  $\beta$ -**CD**. Under neutral conditions, **LA** guests exist in the protonated form. The complexation of  $\beta$ -**CD** with **LA** guests is mainly governed by hydrophobic interactions and by van der Waals interactions.<sup>[20]</sup> The complexation of **SC4A** with **LA** guests is driven by not only C–H⋯π and van der Waals interac-

Table 2. Host–guest stability constants ( $K_S/\text{M}^{-1}$ ) for complexes of **LA** guests with **SC4A**, **CB[7]** and  $\beta$ -**CD**.

Guest	$K_{\text{SC4A}}$	$K_{\text{CB[7]}}$ <sup>[b]</sup>	$K_{\beta\text{-CD}}$
Procaine	$(5.09 \pm 0.08) \times 10^3$	$3.5 \times 10^4$ (pD 4.75)	$1.54 \times 10^3$ <sup>[c]</sup> (uncharged form)
		$4.4 \times 10^5$ (pD 1.0)	$282$ <sup>[c]</sup> (protonated form) $1.4$ <sup>[d]</sup>
Procainamide	$(1.02 \pm 0.01) \times 10^4$	$7.8 \times 10^4$ (pD 4.75)	–
		$5.5 \times 10^4$ (pD 1.0)	–
Tetracaine	$(2.69 \pm 0.05) \times 10^3$	$1.5 \times 10^4$ (pD 4.75)	$6.60 \times 10^3$ <sup>[a]</sup> (uncharged form)
		$1.1 \times 10^6$ (pD 1.0)	$1.36 \times 10^3$ <sup>[a]</sup> (protonated form)
Dibucaine	$(1.79 \pm 0.04) \times 10^4$	$1.8 \times 10^5$ (pD 4.75)	–
		$1.1 \times 10^7$ (pD 1.0)	$6.6 \times 10^2$ <sup>[e]</sup>
Lidocaine	$(6.56 \pm 0.06) \times 10^3$	–	–

[a] Ref.<sup>[22a]</sup> [b] Ref.<sup>[21]</sup> [c] Ref.<sup>[20c]</sup> [d] Ref.<sup>[20b]</sup> [e] Ref.<sup>[20f]</sup>

tions but also by charge interactions between the negatively charged sulfonate groups and the positively charged ammonium group. Similarly, Fernandes et al. reported that **SC6A** forms more stable complexes with tetracaine and proparacaine than  $\beta$ -CD.<sup>[22]</sup> On the other hand, the stability constants of **SC4A** are about two orders of magnitude weaker than those of **CB[7]**. The inner cavity of **CB[7]** offers strong hydrophobic interactions to **LA** guests, and the polar carbonyl groups on the **CB[7]** portals also offers strong dipole–dipole, ion–dipole and hydrogen-bonding interactions to the charged portion of the **LA** guests. It can be seen that **CB[7]** shows the strongest binding affinity to the **LA** guests in the protonated form, whereas  $\beta$ -CD prefers to include **LA** guests with uncharged form.

## Conclusions

We have systematically investigated the binding behavior of three water-soluble calixarenes, **SC4A**, **SC5A**, and **STC4A** with five **LA** guests, procaine, procainamide, tetracaine, dibucaine, and lidocaine. The binding modes depend to a certain extent on the size of the calixarene cavity and on the pH of the solution. <sup>1</sup>H NMR spectra show that, at pD 7.2, **LA** guests are captured by **SCnAs** with the triethylammonium moieties immersed into the cavities of **SCnAs**, except that **STC4A** prefers binding the butylanilinium group of tetracaine. At pD 2.0, **SCnAs** bind the triethylammonium moieties of procaine and procainamide, but unselectively bind the tertiary ammonium and butylanilinium/butyloxy moieties of tetracaine/dibucaine. These observations unambiguously demonstrate that the protonated state of the guest molecule is a crucial factor in the design of supramolecular architectures based on **SCnAs**. Thermodynamically, the complexation of **SCnAs** with the **LA** guests is dominantly driven by the enthalpy term, and the binding abilities enhance continuously with decreasing cavity size. As a result, **SC4A** presents the highest complex constant to **LA** guests, 3 to 7 times larger than **SC5A**, and more than 10 times larger than **STC4A**. Moreover, the differing cavity features of  $\beta$ -CD, **CB[7]**, and **SC4A** results in different binding affinities for **LA** guests. The present results will help to understand the inclusion phenomena and thermodynamic origins of **SCnAs** more systematically and comprehensively, and may provide a potential clinical application in anesthetic studies.

## Experimental Section

**Materials:** The host molecules, *p*-sulfonatocalix[4]arene tetrasodium (**SC4A**),<sup>[36]</sup> *p*-sulfonatothiacalix[4]arene tetrasodium (**STC4A**),<sup>[37]</sup> and *p*-sulfonatocalix[5]arene pentasodium (**SC5A**)<sup>[26b]</sup> were synthesized and purified according to literature procedures. Procaine hydrochloride, procainamide hydrochloride and lidocaine were purchased from Acros (Belgium), the hydrochloride salt of tetracaine was purchased from TCI (Japan), and dibucaine hydrochloride was purchased from Sigma–Aldrich (United States); all were used without further purification. All other chemicals were commercially available, were of reagent grade, and were used with-

out further purification. The phosphate buffer solution of pH 7.2 was prepared by dissolving disodium hydrogen phosphate ( $\text{Na}_2\text{HPO}_4 \cdot 12\text{H}_2\text{O}$ , 25.79 g) and sodium dihydrogen phosphate ( $\text{NaH}_2\text{PO}_4 \cdot 2\text{H}_2\text{O}$ , 4.37 g) in distilled, deionized water (1000 mL) to make a 0.1 M solution. The phosphate  $\text{D}_2\text{O}$  buffer solution of pD 2.0 was prepared by dissolving sodium dihydrogen phosphate ( $\text{NaH}_2\text{PO}_4$ , 0.2379 g) in  $\text{D}_2\text{O}$  (20 mL) to obtain a 0.1 M solution, and then adjusted to pD 2.0 by addition of DCl. The phosphate  $\text{D}_2\text{O}$  buffer solution of pD 7.2 was prepared by dissolving sodium dihydrogen phosphate ( $\text{NaH}_2\text{PO}_4$ , 0.0672 g) and disodium hydrogen phosphate ( $\text{Na}_2\text{HPO}_4$ , 0.2045 g) in  $\text{D}_2\text{O}$  (20 mL) to make a 0.1 M solution. The pH and pD values of buffer solutions were verified with a Sartorius pp-20 pH-meter calibrated with two standard buffer solutions. pH readings were converted into pD units by adding 0.4 units.<sup>[38]</sup>

**General Procedure:** The **LA** guests were added to an aqueous solution of **SCnAs**. The solutions were stirred and adjusted to ca. pH 2 by adding 1 M HCl dropwise. After filtration, the filtrate was allowed to evaporate for several days. The crystals formed were collected together with the mother liquor for the X-ray crystallographic analysis. See the Supporting Information for further details.

**Instruments:** <sup>1</sup>H NMR spectra were recorded at pD 2.0 and 7.2 with a Bruker AV400 spectrometer using 2,2-dimethyl-2-silapentane-5-sulfonate (DSS) as an external reference. The host and the guest were mixed in a 1:1 stoichiometry.

**ITC Measurements:** A thermostatted and fully computer-operated isothermal calorimetry (VP-ITC) instrument, purchased from Microcal Inc. (Northampton, MA), was used for all microcalorimetric experiments. The VP-ITC instrument was calibrated chemically by measurement of the complexation reaction of  $\beta$ -CD with cyclohexanol, and the obtained thermodynamic data were shown to be in good agreement (error less than 2%) with the literature data.<sup>[39]</sup> All microcalorimetric titrations between *p*-sulfonatocalix[*n*]arenes and five local anaesthetics were performed in phosphate

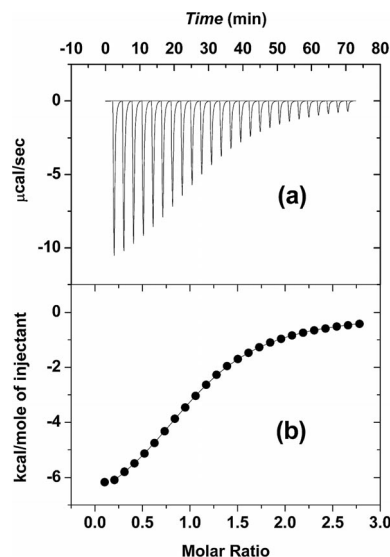


Figure 7. Microcalorimetric titration of procainamide with **SC4A** in phosphate buffer solution (pH 7.2) at 298.15 K. (a) Raw ITC data for sequential 25 injections (10  $\mu\text{L}$  per injection) of procainamide solution (5.77 mM) injecting into **SC4A** solution (0.39 mM). (b) Apparent reaction heat obtained from the integration of calorimetric traces.



buffer solution (pH 7.2) at atmospheric pressure and 298.15 K. Each solution was degassed and thermostatted by a ThermoVac accessory before the titration experiment. Twenty-five successive injections were made for each titration experiment. A constant volume (10  $\mu\text{L}$ /injection) of guest (or host) solution in a 0.250 mL syringe was injected into the reaction cell (1.4227 mL) charged with host (or guest) molecule solution in the same buffer solution. A representative titration curve is shown in Figure 7. As can be seen from Figure 7, each titration of procainamide into the sample cell gave an apparent reaction heat caused by the formation of an inclusion complex between procainamide and SC4A. The reaction heat decreased after each injection of procainamide because fewer SC4A molecules were available to form inclusion complexes. A control experiment was carried out in each run to determine the dilution heat by injecting a guest (or host) buffer solution into a pure phosphate buffer solution containing no host (or guest) molecules. The dilution heat determined in these control experiments was sub-

tracted from the apparent reaction heat measured in the titration experiments to give the net reaction heat.

The net reaction heat in each run was analyzed by using “one set of binding sites” model (ORIGIN software, Microcal Inc.) to simultaneously compute the binding stoichiometry ( $N$ ), complex stability constant ( $K_S$ ), standard molar reaction enthalpy ( $\Delta H^\circ$ ), and standard deviation from the titration curve. Generally, the first point of the titration curve was disregarded, as some liquid mixing near the tip of the injection needle is known to occur at the beginning of each ITC run. Knowledge of the complex stability constant ( $K_S$ ) and molar reaction enthalpy ( $\Delta H^\circ$ ) enabled calculation of the standard free energy ( $\Delta G^\circ$ ) and entropy changes ( $\Delta S^\circ$ ) according to

$$\Delta G^\circ = -RT \ln K_S = \Delta H^\circ - T\Delta S^\circ$$

where  $R$  is the gas constant and  $T$  is the absolute temperature.

A typical curve fitting result for the complexation of procainamide with SC4A in phosphate buffer solution (pH 7.2) is shown in Figure 8. To check the accuracy of the observed thermodynamic parameters, two independent titration experiments were carried out to afford self-consistent thermodynamic parameters, and their average values with associated errors are listed in Table 1.

**Supporting Information** (see footnote on the first page of this article): Chemical shift changes of LA guests in the presence of SCnAs;  $^1\text{H}$  NMR spectra of LA guests in the absence and presence of SCnAs under neutral and acid conditions; Experimental details for the preparation of solid-state complexes; Crystal structure data and details of the structure refinements for complexes.

## Acknowledgment

This work was supported by the Ministry of Science and Technology (MOST) (973 Program, grant number 2011CB932502) and the National Natural Science Foundation of China (NSFC) (grant numbers 20932004 and 21172119), which are gratefully acknowledged.

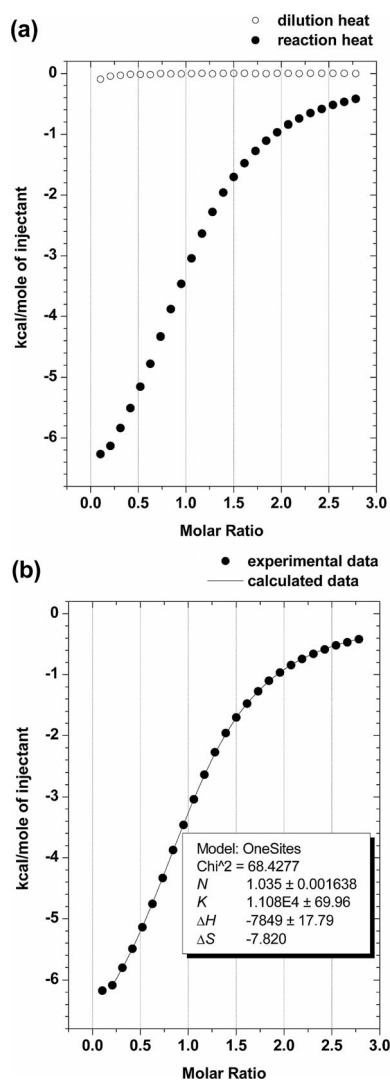


Figure 8. (a) Heat effects of the dilution and of the complexation reaction of procainamide with SC4A for each injection during titration microcalorimetric experiment. (b) “Net” heat effects of complexation of procainamide with SC4A for each injection, obtained by subtracting the dilution heat from the reaction heat, which was fitted by computer simulation using the “one set of binding sites” model.

- [1] a) C. D. Gutsche, in: *Monographs in Supramolecular Chemistry* (Ed.: J. F. Stoddart), *Calixarenes Revisited*, Royal Society of Chemistry, Cambridge, U. K., **1998**, p. 112; b) V. Böhmer, *Angew. Chem.* **1995**, *107*, 785; *Angew. Chem. Int. Ed. Engl.* **1995**, *34*, 713–745; c) A. Ikeda, S. Shinkai, *Chem. Rev.* **1997**, *97*, 1713–1734.
- [2] F. Perret, A. N. Lazar, A. W. Coleman, *Chem. Commun.* **2006**, 2425–2438.
- [3] a) J.-P. Morel, N. Morel-Desrosiers, *Org. Biomol. Chem.* **2006**, *4*, 462–465; b) D. Cuc, S. Bouguet-Bonnet, N. Morel-Desrosiers, J.-P. Morel, P. Nutzenhardt, D. Canet, *J. Phys. Chem. B* **2009**, *113*, 10800–10807; c) N. Basilio, L. García-Río, M. Martín-Paster, *J. Phys. Chem. B* **2010**, *114*, 7201–7206.
- [4] a) M. Baur, M. Frank, J. Schatz, F. Schildbach, *Tetrahedron* **2001**, *57*, 6985–6991; b) G. Arena, A. Contino, F. G. Gulino, A. Magri, D. Sciotto, R. Ungaro, *Tetrahedron Lett.* **2000**, *41*, 9327–9330; c) N. Kon, N. Iki, S. Miyano, *Org. Biomol. Chem.* **2003**, *1*, 751–755; d) H. Bakirci, A. L. Koner, W. M. Nau, *J. Org. Chem.* **2005**, *70*, 9960–9966.
- [5] a) S. Shinkai, K. Araki, T. Matsuda, N. Nishiyama, H. Ikeda, I. Takasu, M. Iwamoto, *J. Am. Chem. Soc.* **1990**, *112*, 9053–9058; b) G. Arena, A. Casnati, A. Contino, G. G. Lombardo, D. Sciotto, R. Ungaro, *Chem. Eur. J.* **1999**, *5*, 738–744; c) G. Arena, S. Gentile, F. G. Gulino, D. Sciotto, C. Sgarlata, *Tetrahedron Lett.* **2004**, *45*, 7091–7094; d) A. Ghoufi, C. Bonal, J. P. Morel, N. Morel-Desrosiers, P. Malfreyt, *J. Phys. Chem. B* **2004**, *108*, 5095–5104.

- [6] a) Y. Liu, D.-S. Guo, E.-C. Yang, H.-Y. Zhang, Y.-L. Zhao, *Eur. J. Org. Chem.* **2005**, 162–170; b) Y. Liu, E.-C. Yang, Y. Chen, D.-S. Guo, F. Ding, *Eur. J. Org. Chem.* **2005**, 4581–4588; c) Y. Liu, D.-S. Guo, H.-Y. Zhang, Y.-H. Ma, E.-C. Yang, *J. Phys. Chem. B* **2006**, *110*, 3428–3434; d) Y. Liu, Y.-H. Ma, Y. Chen, D.-S. Guo, Q. Li, *J. Org. Chem.* **2006**, *71*, 6468–6473; e) D.-S. Guo, L.-H. Wang, Y. Liu, *J. Org. Chem.* **2007**, *72*, 7775–7778; f) C. Gaeta, T. Caruso, M. Mincoletti, F. Troisi, E. Vasca, P. Neri, *Tetrahedron* **2008**, *64*, 5370–5378.
- [7] a) K. N. Koh, K. Araki, A. Ikeda, H. Otsuka, S. Shinkai, *J. Am. Chem. Soc.* **1996**, *118*, 755–758; b) N. Douteau-Guével, F. Perret, A. W. Coleman, J.-P. Morel, N. Morel-Desrosiers, *J. Chem. Soc. Perkin Trans. 2* **2002**, 524–532; c) G. Arena, A. Casnati, A. Contino, A. Magri, F. Sansone, D. Sciotto, R. Ungaro, *Org. Biomol. Chem.* **2006**, *4*, 243–249; d) M. Megyesi, L. Biczók, *Chem. Phys. Lett.* **2006**, *424*, 71–76; e) W. Yang, M. M. De Villiers, *Eur. J. Pharm. Biopharm.* **2004**, *58*, 629–636; f) M. Megyesi, L. Biczók, *J. Phys. Chem. B* **2010**, *114*, 2814–2819.
- [8] a) S. Shinkai, K. Araki, T. Matsuda, O. Manabe, *Bull. Chem. Soc. Jpn.* **1989**, *62*, 3856–3862; b) G. Arena, A. Casnati, A. Contino, F. G. Gulino, D. Sciotto, R. Ungaro, *J. Chem. Soc. Perkin Trans. 2* **2000**, 419–423; c) A. Mendes, C. Bonal, N. Morel-Desrosiers, J.-P. Morel, P. Malfreyt, *J. Phys. Chem. B* **2002**, *106*, 4516–4524; d) H. Bakirci, W. M. Nau, *Adv. Funct. Mater.* **2006**, *16*, 237–242; e) V. Souchon, I. Leray, B. Valeur, *Chem. Commun.* **2006**, 4224–4226; f) D. Xiong, M. Chen, H. Li, *Chem. Commun.* **2008**, 880–882.
- [9] a) G. W. Orr, L. J. Barbour, J. L. Atwood, *Science* **1999**, *285*, 1049–1052; b) J. L. Atwood, L. J. Barbour, S. J. Dalgarno, M. J. Hardie, C. L. Raston, H. R. Webb, *J. Am. Chem. Soc.* **2004**, *126*, 13170–13171; c) J. L. Atwood, L. J. Barbour, M. J. Hardie, C. L. Raston, *Coord. Chem. Rev.* **2001**, *222*, 3–32; d) S. J. Dalgarno, J. L. Atwood, C. L. Raston, *Chem. Commun.* **2006**, 4567–4574; e) O. Danylyuk, K. Suwinska, *Chem. Commun.* **2009**, 5799–5813; f) I. Ling, Y. Alias, C. L. Raston, *New J. Chem.* **2010**, *34*, 1802–1811.
- [10] a) S. Shinkai, S. Mori, H. Koreishi, T. Tsubaki, O. Manabe, *J. Am. Chem. Soc.* **1986**, *108*, 2409–2416; b) K. Goto, Y. Yano, E. Okada, C.-W. Liu, K. Yamamoto, R. Ueoka, *J. Org. Chem.* **2003**, *68*, 865–870; c) R. Kaliappan, L. S. Kaanumalle, A. Natarajan, V. Ramamurthy, *Photochem. Photobiol. Sci.* **2006**, *5*, 925–930; d) Y.-L. Liu, L. Liu, Y.-L. Wang, Y.-C. Han, D. Wang, Y.-J. Chen, *Green Chem.* **2008**, *10*, 635–640.
- [11] a) S. Houmadi, D. Coquière, L. Legrand, M. C. Fauré, M. Goldmann, O. Reinaud, S. Rémita, *Langmuir* **2007**, *23*, 4849–4855; b) N. Basilio, L. García-Río, *Chem. Eur. J.* **2009**, *15*, 9315–9319; c) V. Francisco, N. Basilio, L. García-Río, J. R. Leis, E. F. Maques, C. Vázquez-Vázquez, *Chem. Commun.* **2010**, *46*, 6551–6553; d) K. Wang, D.-S. Guo, Y. Liu, *Chem. Eur. J.* **2010**, *16*, 8006–8011.
- [12] F. Perret, A. W. Coleman, *Chem. Commun.* **2011**, *47*, 7303–7319.
- [13] A. W. Coleman, A. N. Lazar, K. Suwinska, O. Danylyuk, *World Pat. PCT/FR2007/051129*, **2007**.
- [14] W. Yang, D. P. Daniel, W. Liebenberg, M. M. de Villiers, *Curr. Drug Discovery Technol.* **2008**, *5*, 129–139.
- [15] K. Wang, D.-S. Guo, Y. Liu, *J. Med. Chem.* **2009**, *52*, 6402–6412.
- [16] G.-S. Wang, H.-Y. Zhang, F. Ding, Y. Liu, *J. Inclusion Phenom. Macrocyclic Chem.* **2011**, *69*, 85–89.
- [17] G.-S. Wang, H.-Y. Zhang, D. Li, P.-Y. Wang, Y. Liu, *Supramol. Chem.* **2011**, *23*, 441–446.
- [18] M. Chorny, R. J. Levy, *Proc. Natl. Acad. Sci. USA* **2009**, *106*, 6891–6892.
- [19] P. M. Friedman, E. A. Mafong, E. S. Friedman, R. G. Geronemus, *Dermatol. Surg.* **2001**, *27*, 1019–1026.
- [20] a) C. Merino, E. Junquera, J. Jiménez-Barbero, E. Aicart, *Langmuir* **2000**, *16*, 1557–1565; b) E. Iglesias, *J. Org. Chem.* **2006**, *71*, 4383–4392; c) E. Iglesias-Martínez, I. Brandariz, F. Penedo, *J. Inclusion Phenom. Macrocyclic Chem.* **2007**, *57*, 573–576; d) M. A. Deryabina, S. H. Hansen, J. Østergaard, H. Jensen, *J. Phys. Chem. B* **2009**, *113*, 7263–7269; e) I. Brandariz, E. Iglesias-Martínez, *J. Chem. Eng. Data* **2009**, *54*, 2103–2105; f) N. Takisawa, K. Shirahama, I. Tanaka, *Colloid Polym. Sci.* **1993**, *271*, 499–506.
- [21] I. W. Wyman, D. H. Macartney, *Org. Biomol. Chem.* **2010**, *8*, 247–252.
- [22] a) S. A. Fernandes, L. F. Cabeça, A. J. Marsaioli, E. de Paula, *J. Inclusion Phenom. Macrocyclic Chem.* **2007**, *57*, 395–401; b) L. M. Arantes, C. Scarelli, A. J. Marsaioli, E. de Paula, S. A. Fernandes, *Magn. Reson. Chem.* **2009**, *47*, 757–763.
- [23] O. Danylyuk, M. Monachino, A. N. Lazar, K. Suwinska, A. W. Coleman, *J. Mol. Struct.* **2010**, *965*, 116–120.
- [24] a) J. L. Atwood, L. J. Barbour, S. J. Dalgarno, C. L. Raston, H. R. Webb, *J. Chem. Soc., Dalton Trans.* **2002**, 4351–4356; b) S. J. Dalgarno, J. L. Atwood, C. L. Raston, *Cryst. Growth Des.* **2006**, *6*, 174–180; c) Y. Liu, K. Chen, D.-S. Guo, Q. Li, H.-B. Song, *Cryst. Growth Des.* **2007**, *7*, 2601–2608.
- [25] N. Iki, T. Suzuki, K. Koyama, C. Kabuto, S. Miyano, *Org. Lett.* **2002**, *4*, 509–512.
- [26] a) H. Matsumiya, Y. Terazono, N. Iki, S. Miyano, *J. Chem. Soc. Perkin Trans. 2* **2002**, 1166–1172; b) J. W. Steed, C. P. Johnson, C. L. Barnes, R. K. Juneja, J. L. Atwood, S. Reilly, R. L. Hollis, P. H. Smith, D. L. Clark, *J. Am. Chem. Soc.* **1995**, *117*, 11426–11433.
- [27] C. Bonal, Y. Israëli, J.-P. Morel, N. Morel-Desrosiers, *J. Chem. Soc. Perkin Trans. 2* **2001**, 1075–1078.
- [28] N. Douteau-Guével, A. W. Coleman, J.-P. Morel, N. Morel-Desrosiers, *J. Chem. Soc. Perkin Trans. 2* **1999**, 629–634.
- [29] J. Cui, V. D. Uzunova, D.-S. Guo, K. Wang, W. M. Nau, Y. Liu, *Eur. J. Org. Chem.* **2010**, 1704–1710.
- [30] D.-S. Guo, H.-Q. Zhang, F. Ding, Y. Liu, *Org. Biomol. Chem.* **2012**, *10*, 1527–1536.
- [31] W. Tao, M. Barra, *J. Chem. Soc. Perkin Trans. 2* **1998**, 1957–1960.
- [32] Y. Liu, Y. Chen, *Acc. Chem. Res.* **2006**, *39*, 681–691.
- [33] J. Lagona, P. Mukhopadhyay, S. Chakrabarti, L. Isaacs, *Angew. Chem.* **2005**, *117*, 4922; *Angew. Chem. Int. Ed.* **2005**, *44*, 4844–4870.
- [34] M. K. Singh, H. Pal, A. S. R. Koti, A. V. Sapre, *J. Phys. Chem. A* **2004**, *108*, 1465–1474.
- [35] a) J. W. Lee, S. Samal, N. Selvapalam, H.-J. Kim, K. Kim, *Acc. Chem. Res.* **2003**, *36*, 621–630; b) K. Kim, *Chem. Soc. Rev.* **2002**, *31*, 96–107; c) C. Márquez, R. R. Hudgins, W. M. Nau, *J. Am. Chem. Soc.* **2004**, *126*, 5806–5816.
- [36] G. Arena, A. Contino, G. G. Lombardo, D. Sciotto, *Thermochim. Acta* **1995**, *264*, 1–11.
- [37] N. Iki, T. Fujimoto, S. Miyano, *Chem. Lett.* **1998**, 625–626.
- [38] P. K. Glasoe, F. A. Long, *J. Phys. Chem.* **1960**, *64*, 188–190.
- [39] M. V. Rekharsky, Y. Inoue, *Chem. Rev.* **1998**, *98*, 1875–1917.

Received: April 19, 2012  
Published Online: June 12, 2012